Electronic Supplementary Material (ESI) for Dalton Transactions

Supporting Information

Polyoxometalate-templated lanthanide-organic hybrid layers based on 6^3-honeycomb-like 2D nets

Xiu-Li Hao,[a] Ming-Fa Luo,[a] Wei Yao,[a] Yang-Guang Li,[*a] Yong-Hui Wang[*a] and En-Bo Wang[a]

Contents

1 Additional structural figures for compounds **1, 2 and 3**

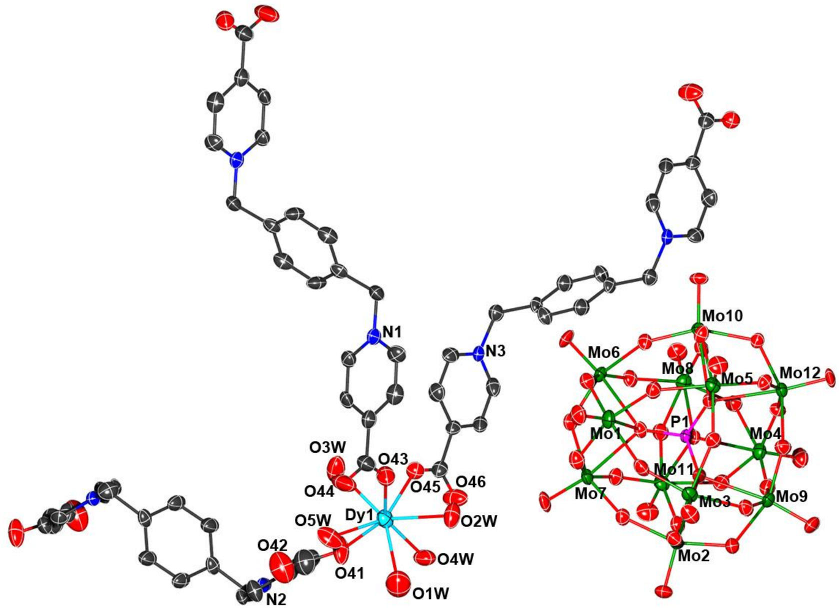

Fig. S1 ORTEP diagram of the basic structural units in **compound 1** with thermal ellipsoids at 30% probability displacement. All H atoms and solvent molecules are omitted for clarity.

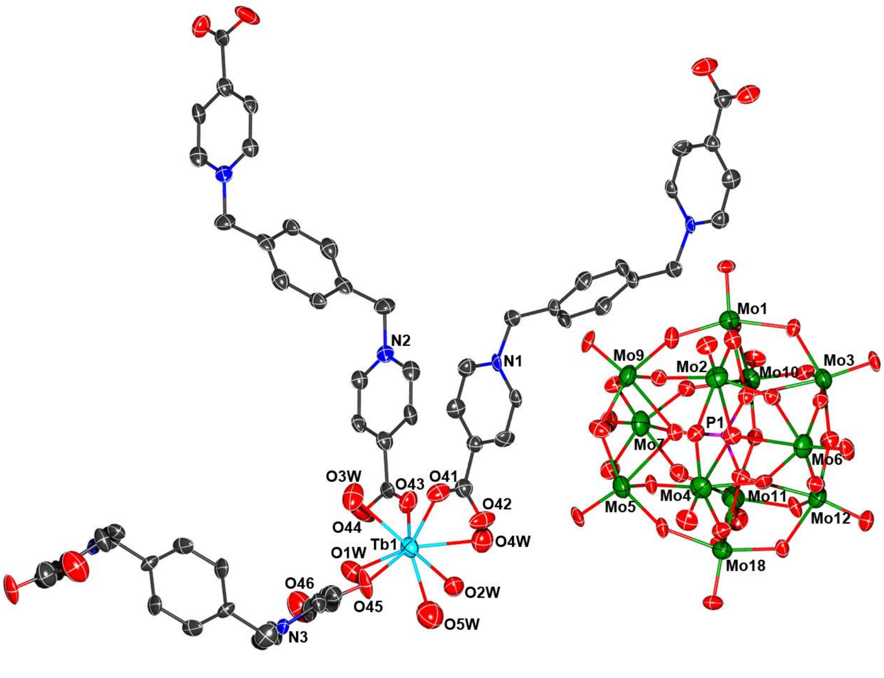

Fig. S2 ORTEP diagram of the basic structural units in **compound 2** with thermal ellipsoids at 30% probability displacement. All H atoms and solvent molecules are omitted for clarity.

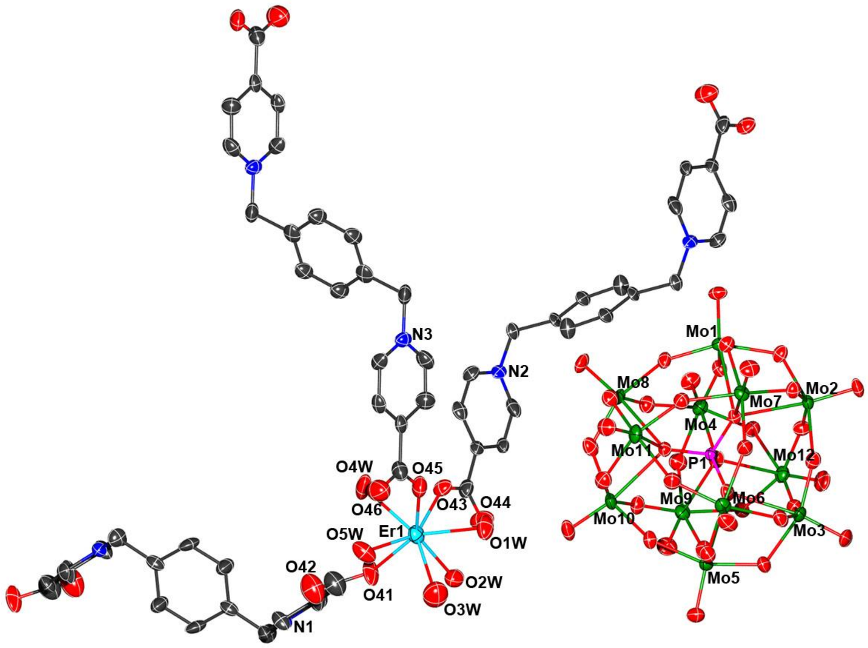

Fig. S3 ORTEP diagram of the basic structural units in **compound 3** with thermal ellipsoids at 30% probability displacement. All H atoms and solvent molecules are omitted for clarity.

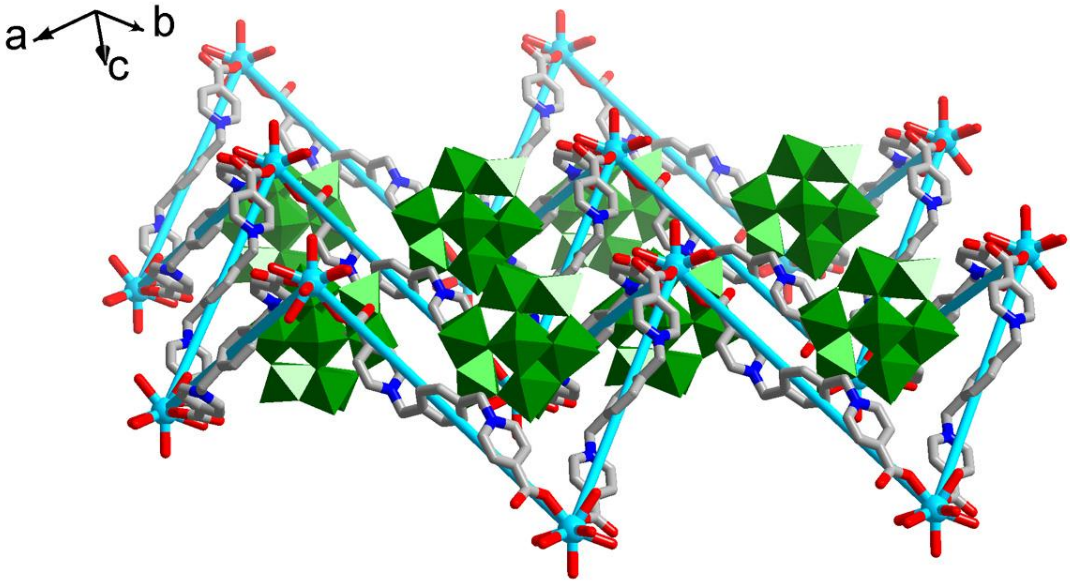

Fig. S4 The side view of the cationic 2D lanthanide-organic network in **1** and the distribution of Keggin-type POM templates in the layer.

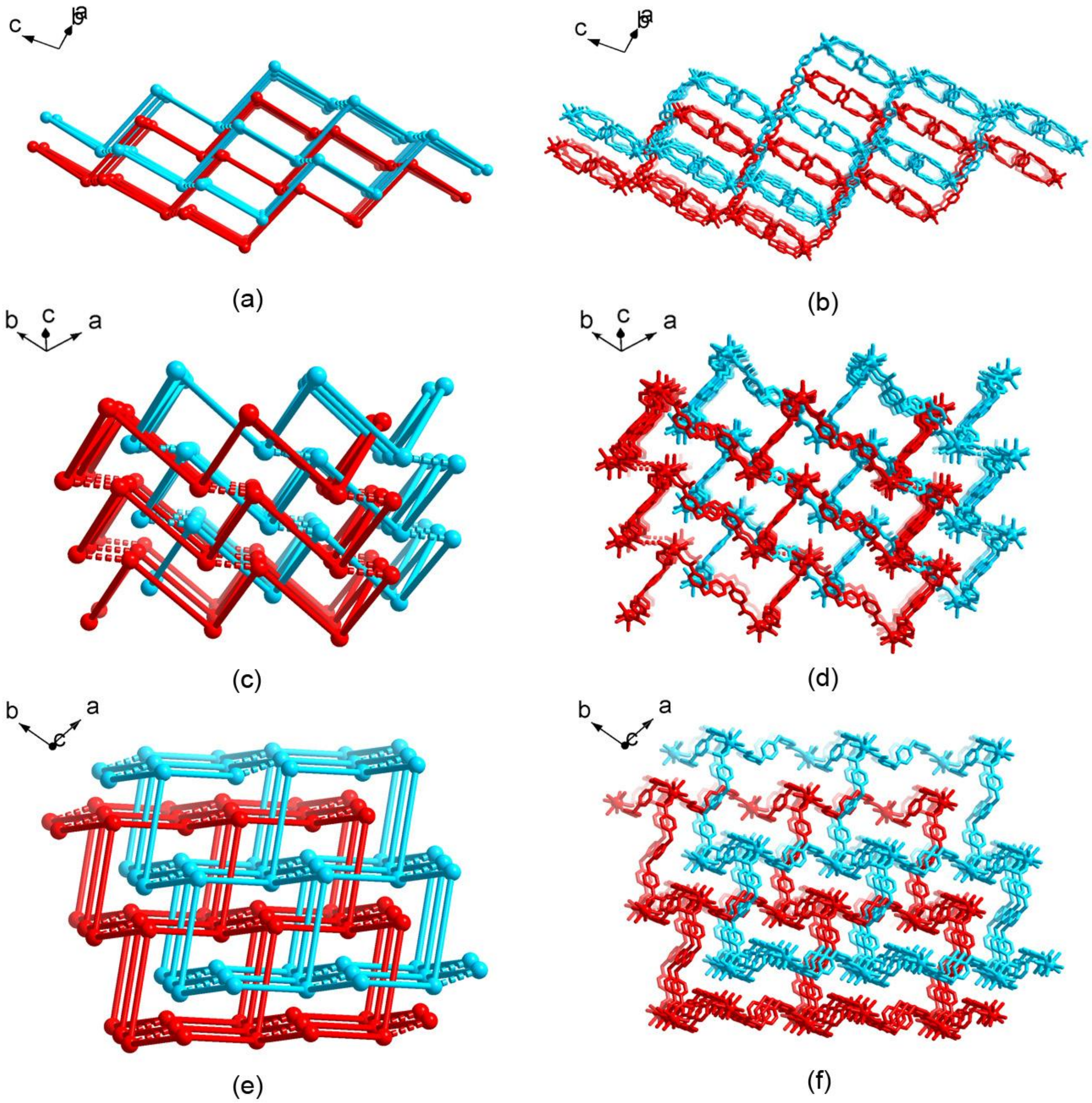

Fig. S5 (a) (c) (e) The schematic views of the H-bonding interactions between two interval layers and the 2-fold interpenetrating supramolecular framework in **1**; **(b) (d) (f)** The relevant structural features of the 3D entangled lanthanide-organic supramolecular framework in **1**.

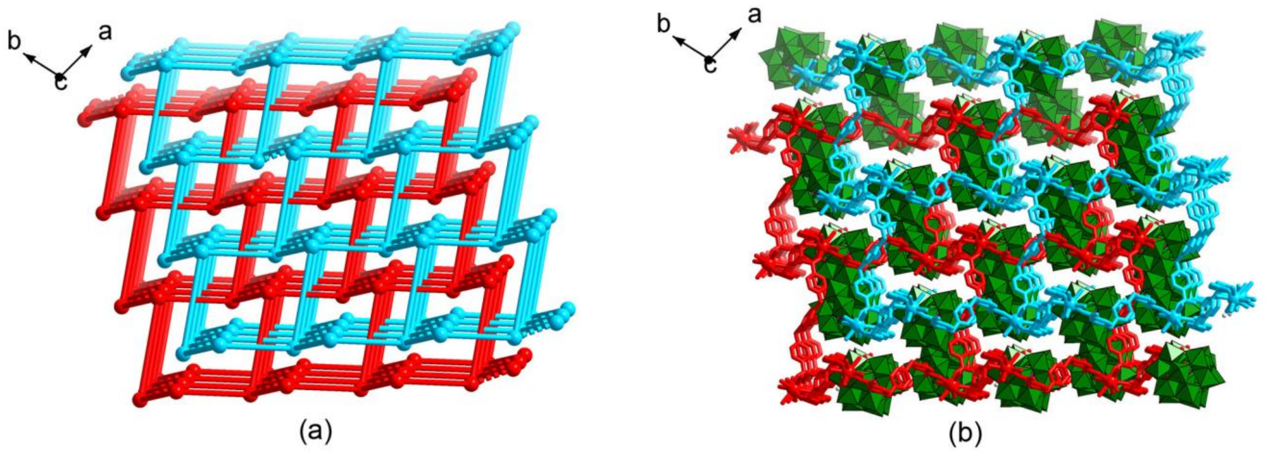

Fig. S6 (a) Schematic view of the 3D lanthanide-organic supramolecular framework in **1** with the two-fold interpenetration mode; **(b)** the distribution of POM templates in the lanthanide-organic supramolecular framework viewed along *c* axis.

2 Selected bond lengths and angles for compounds **1**, **2 and 3**

Table S1. Selected bond lengths (Å) and angles (deg) of compound **1**

Dy(1)-O(41)	2.237(12)	Dy(1)-O(43)	2.270(10)
Dy(1)-O(45)	2.345(9)	Dy(1)-O(1W)	2.386(13)
Dy(1)-O(2W)	2.367(11)	Dy(1)-O(3W)	2.384(11)
Dy(1)-O(4W)	2.389(10)	Dy(1)-O(5W)	2.387(12)
O(41)-Dy(1)-O(43)	140.0(4)	O(41)-Dy(1)-O(45)	103.4(4)
O(41)-Dy(1)-O(1W)	86.4(5)	O(41)-Dy(1)-O(2W)	147.2(4)
O(41)-Dy(1)-O(3W)	74.4(5)	O(41)-Dy(1)-O(4W)	73.7(4)
O(41)-Dy(1)-O(5W)	74.7(4)	O(43)-Dy(1)-O(45)	92.1(4)
O(43)-Dy(1)-O(1W)	104.7(5)	O(43)-Dy(1)-O(2W)	71.8(4)
O(43)-Dy(1)-O(3W)	76.5(4)	O(43)-Dy(1)-O(4W)	146.2(4)
O(43)-Dy(1)-O(5W)	73.1(4)	O(45)-Dy(1)-O(1W)	140.5(4)
O(45)-Dy(1)-O(2W)	77.4(4)	O(45)-Dy(1)-O(3W)	70.8(3)
O(45)-Dy(1)-O(4W)	75.5(3)	O(45)-Dy(1)-O(5W)	148.4(3)
O(1W)-Dy(1)-O(2W)	74.5(5)	O(1W)-Dy(1)-O(3W)	147.5(5)
O(1W)-Dy(1)-O(4W)	70.8(5)	O(1W)-Dy(1)-O(5W)	71.1(5)
O(2W)-Dy(1)-O(3W)	133.6(4)	O(2W)-Dy(1)-O(4W)	74.9(4)
O(2W)-Dy(1)-O(5W)	121.5(4)	O(3W)-Dy(1)-O(4W)	125.8(4)
O(3W)-Dy(1)-O(5W)	78.5(4)	O(4W)-Dy(1)-O(5W)	131.3(4)

Symmetry transformations used to generate equivalent atoms: #1 -x+1,-y+1,-z; #2 -x,-y+2,-z; #3 -x-1,-y+1,-z+1

Table S2. Selected bond lengths (Å) and angles (deg) of compound **2**

Tb(1)-O(41)	2.370(12)	Tb(1)-O(43)	2.262(15)
Tb(1)-O(45)	2.254(13)	Tb(1)-O(1W)	2.386(14)
Tb(1)-O(2W)	2.447(15)	Tb(1)-O(3W)	2.419(14)
Tb(1)-O(4W)	2.420(15)	Tb(1)-O(5W)	2.398(17)
O(41)-Tb(1)-O(43)	91.9(5)	O(41)-Tb(1)-O(45)	102.5(5)
O(41)-Tb(1)-O(1W)	148.8(5)	O(41)-Tb(1)-O(2W)	75.1(5)
O(41)-Tb(1)-O(3W)	71.2(5)	O(41)-Tb(1)-O(4W)	77.4(5)
O(41)-Tb(1)-O(5W)	139.4(6)	O(43)-Tb(1)-O(45)	141.4(5)
O(43)-Tb(1)-O(1W)	73.5(5)	O(43)-Tb(1)-O(2W)	146.5(5)
O(43)-Tb(1)-O(3W)	76.2(5)	O(43)-Tb(1)-O(4W)	71.6(5)
O(43)-Tb(1)-O(5W)	104.8(6)	O(45)-Tb(1)-O(1W)	76.0(5)
O(45)-Tb(1)-O(2W)	72.1(5)	O(45)-Tb(1)-O(3W)	75.0(6)
O(45)-Tb(1)-O(4W)	146.3(6)	O(45)-Tb(1)-O(5W)	87.2(6)
O(1W)-Tb(1)-O(2W)	131.1(5)	O(1W)-Tb(1)-O(3W)	78.4(5)
O(1W)-Tb(1)-O(4W)	121.4(5)	O(1W)-Tb(1)-O(5W)	71.8(6)
O(2W)-Tb(1)-O(3W)	125.6(5)	O(2W)-Tb(1)-O(4W)	75.4(5)
O(2W)-Tb(1)-O(5W)	70.7(6)	O(3W)-Tb(1)-O(4W)	133.6(5)
O(3W)-Tb(1)-O(5W)	148.2(6)	O(4W)-Tb(1)-O(5W)	73.6(6)

Symmetry transformations used to generate equivalent atoms: #1 -x+1,-y+2,-z+1; #2 -x+2,-y+1,-z+1; #3 -x+3,-y+2,-z; #4 -x+2,-y+1,-z

Table S3. Selected bond lengths (Å) and angles (deg) of compound **3**

Er(1)-O(41)	2.240(11)	Er(1)-O(43)	2.343(10)
Er(1)-O(45)	2.242(14)	Er(1)-O(1W)	2.319(12)
Er(1)-O(2W)	2.392(13)	Er(1)-O(3W)	2.339(15)
Er(1)-O(4W)	2.364(12)	Er(1)-O(5W)	2.347(12)
O(41)-Er(1)-O(43)	103.0(5)	O(41)-Er(1)-O(45)	141.7(5)
O(41)-Er(1)-O(1W)	145.7(5)	O(41)-Er(1)-O(2W)	71.7(5)
O(41)-Er(1)-O(3W)	89.6(6)	O(41)-Er(1)-O(4W)	75.3(6)
O(41)-Er(1)-O(5W)	75.3(5)	O(43)-Er(1)-O(45)	92.0(4)
O(43)-Er(1)-O(1W)	77.4(4)	O(43)-Er(1)-O(2W)	76.4(4)
O(43)-Er(1)-O(3W)	140.6(5)	O(43)-Er(1)-O(4W)	70.9(4)
O(43)-Er(1)-O(5W)	148.8(4)	O(45)-Er(1)-O(1W)	71.8(5)
O(45)-Er(1)-O(2W)	146.7(4)	O(45)-Er(1)-O(3W)	100.9(6)
O(45)-Er(1)-O(4W)	76.7(5)	O(45)-Er(1)-O(5W)	73.9(4)
O(1W)-Er(1)-O(2W)	75.2(5)	O(1W)-Er(1)-O(3W)	71.8(5)
O(1W)-Er(1)-O(4W)	133.9(5)	O(1W)-Er(1)-O(5W)	121.8(5)
O(2W)-Er(1)-O(3W)	72.4(5)	O(2W)-Er(1)-O(4W)	126.0(5)
O(2W)-Er(1)-O(5W)	130.3(4)	O(3W)-Er(1)-O(4W)	148.2(5)
O(3W)-Er(1)-O(5W)	70.4(5)	O(4W)-Er(1)-O(5W)	78.7(4)

Symmetry transformations used to generate equivalent atoms: #1 -x-1,-y+1,-z+1; #2 -x+1,-y+1,-z; #3 -x,-y+2,-z

3 Additional physical measurements for compounds **1, 2 and 3**

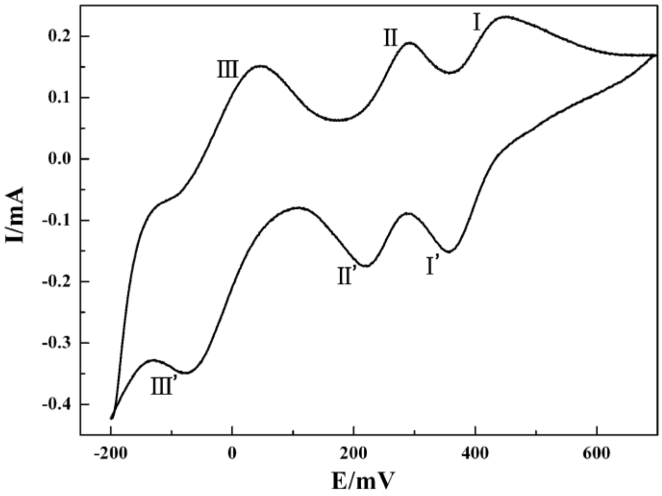

Fig. S7 Cyclic voltammogram of **1-**CPE in a 1M H_2SO_4 solution at a scan rate of 100 mV/s; the reference electrode was Ag/AgCl.

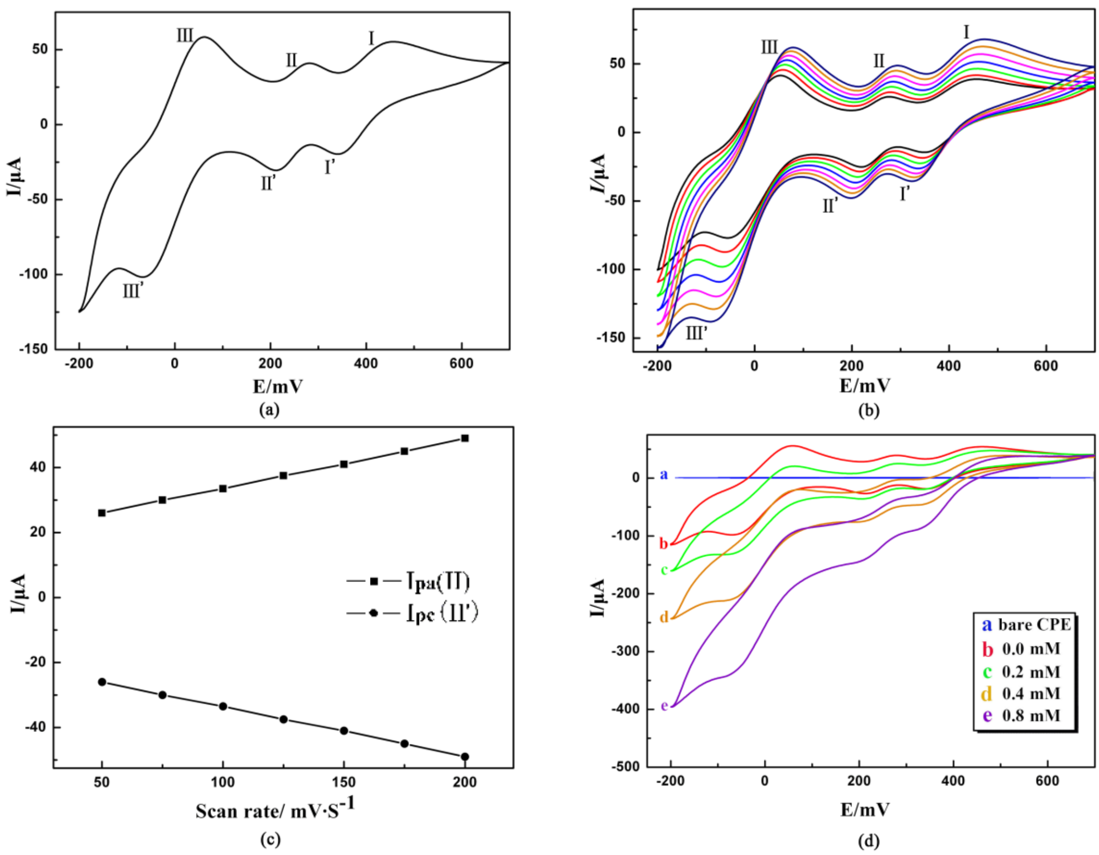

Fig. S8 (a) Cyclic voltammograms (CV) of **2-**CPE in 1 M H_2SO_4 at scan rate of 100 mV/s, the reference electrode was Ag/AgCl; **(b)** CVs of the **2-CPE** in 1 M H_2SO_4 at different scan rates (from inner to outer: 50, 75, 100, 125, 150, 175 and 200 mV/s); **(c)** plots of the dependence of anodic peak and cathodic peak (II–II') current on scan rate; **(d)** CVs of **2-CPE** in 1 M H_2SO_4 containing 0.0-0.8 mM KNO_2 and a bare CPE in 0.50 mM KNO_2 + 1 M H_2SO_4 solution.

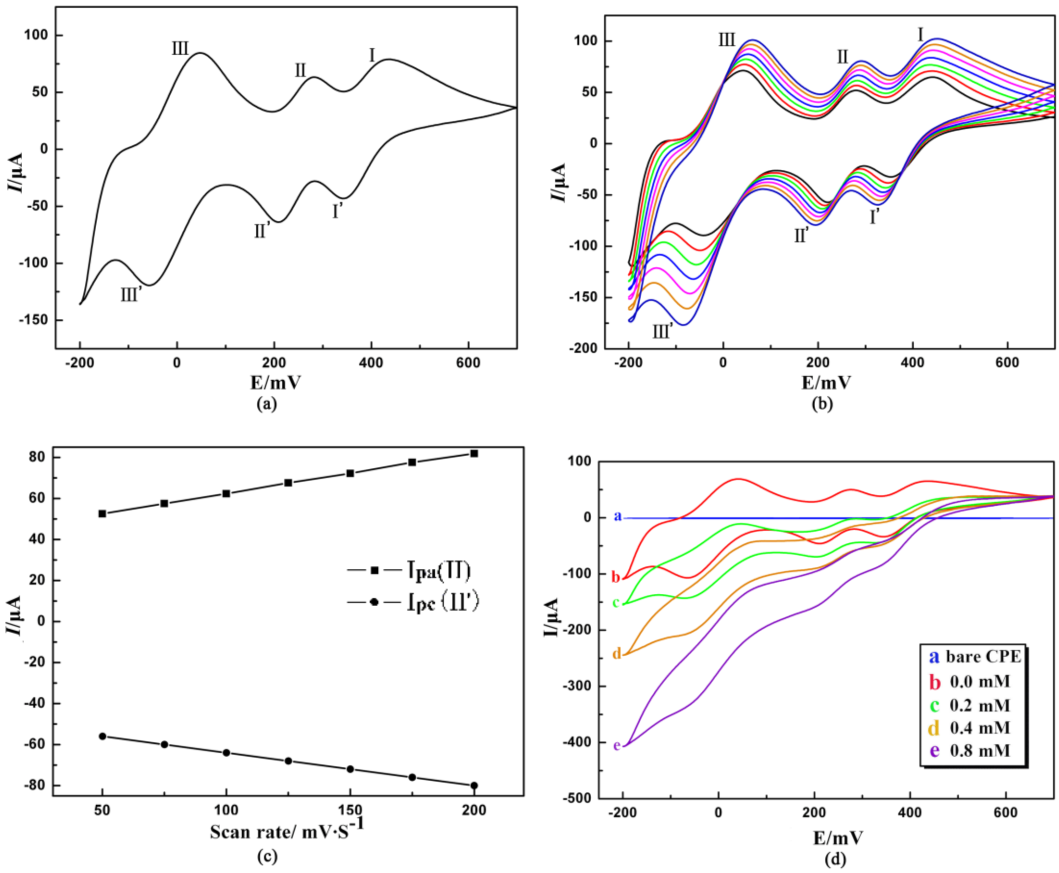

Fig. S9 (a) Cyclic voltammogram (CV) of **3-**CPE in the 1 M H_2SO_4 solution at a scan rate of 100 mV/s; the reference electrode was Ag/AgCl; **(b)** CVs of **3-CPE** in 1 M H_2SO_4 at different scan rates (from inner to outer: 50, 75, 100, 125, 150, 175 and 200 mV/s); **(c)** plots of the dependence of anodic peak and cathodic peak (II–II') current on scan rate; **(d)** CVs of **3-CPE** in 1 M H_2SO_4 containing 0.0-0.8 mM KNO_2 and a bare CPE in 0.50 mM KNO_2 + 1 M H_2SO_4 solution.

IR spectra

The IR spectra of compounds **1-3** show four characteristic peaks of the polyoxoanion $[PMo_{12}O_{40}]^{3-}$ in the range of 1000-700 cm^{-1}. The peaks at ca. 1063 cm^{-1}, 957 cm^{-1}, 878 cm^{-1}, and 800 cm^{-1} are ascribed to the vibrations of *v*(P-O), *v*(Mo=$O_{terminal}$) and *v*(Mo–O_{bridge}–Mo), respectively. [4a] In addition, characteristic bands at ca. 1634 and 1384 cm^{-1} are the vibrations of the v_{as}(-COO) and v_s(-COO) in L ligand, respectively. The peaks at ca. 3118 and 3059 cm^{-1} are attributed to the vibrations of the *v*(C-H) in phenyl and pyridyl rings of L ligand. Peaks in the regions of 1570-1457 cm^{-1} may belong to the vibrations of the *v*(C=C) in phenyl and pyridyl rings of L ligand. The peaks at ca. 3436 cm^{-1} are attributed to the vibrations of *v*(H_2O).

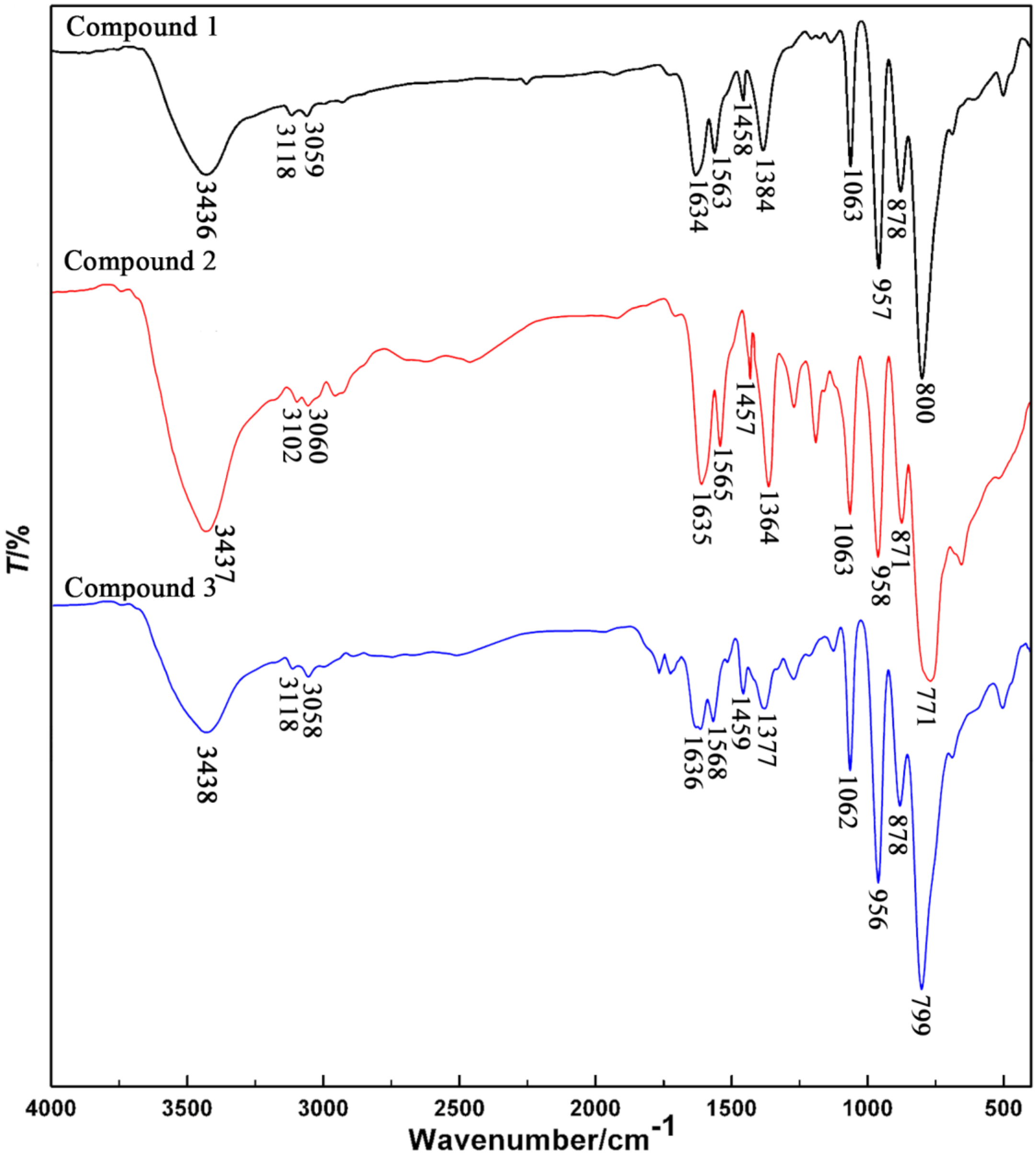

Fig. S10. IR spectra of compound **1** (black), compound 2 (red) and compound 3 (blue) measured at room temperature.

TG Analyses

The TG curve of compound **1** shows two continuous weight loss steps (Fig. S11). The first weight loss of 6.90 % in the temperature range of 45 ~ 212°C corresponds to the loss of the solvent acetonitrile and water molecules as well as five coordinated water molecules (calcd. 6.96%). The second weight loss of 19.60% occurring from 212 to 535 °C is mainly ascribed to the decomposition and loss of L ligands (calcd. 19.37%). The whole weight loss of 26.50 % is in agreement with the calculated value 26.33%.

The TG curve of compound **2** (Fig. S12) shows the first weight loss of 6.85 % from 45 to 221 °C, which is assigned to the removal of all solvent acetonitrile and water molecules together with five coordinated water molecules (calcd. 6.97 %). The second weight loss of 19.60 % from 221 to 536 °C is ascribed to decomposition and loss of L ligands (calcd. 19.39%). The whole weight loss of 26.45% is in agreement with the calculated value 26.36%.

The TG curve of compound **3** also shows two continuous weight loss steps (Fig. S13). The first weight loss of 6.75 % in the temperature range of 45 ~ 220 °C corresponds to the loss of solvent acetonitrile and water molecules as well as five coordinated water molecules (calcd. 6.94%). The second weight loss in the range of 220 ~ 553 °C is 19.45% and attributed to the loss of L ligands (calcd. 19.34%). The whole weight loss of 26.20 % is in agreement with the calculated value 26.28%.

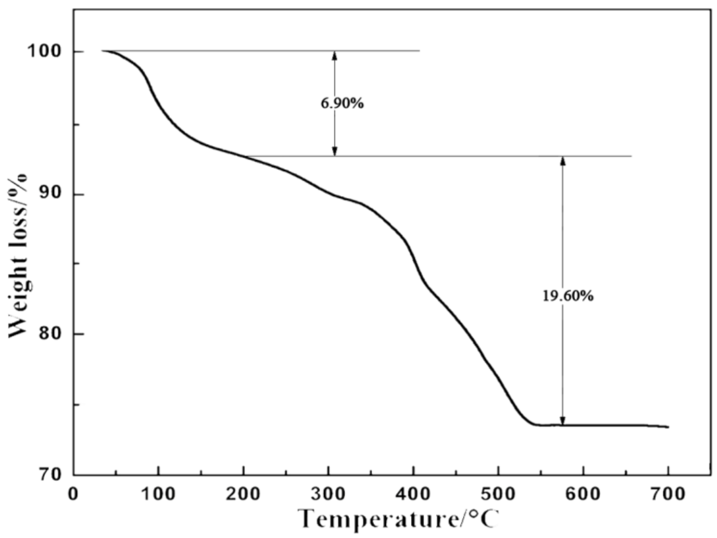

Fig. S11 TG curve of compound **1**

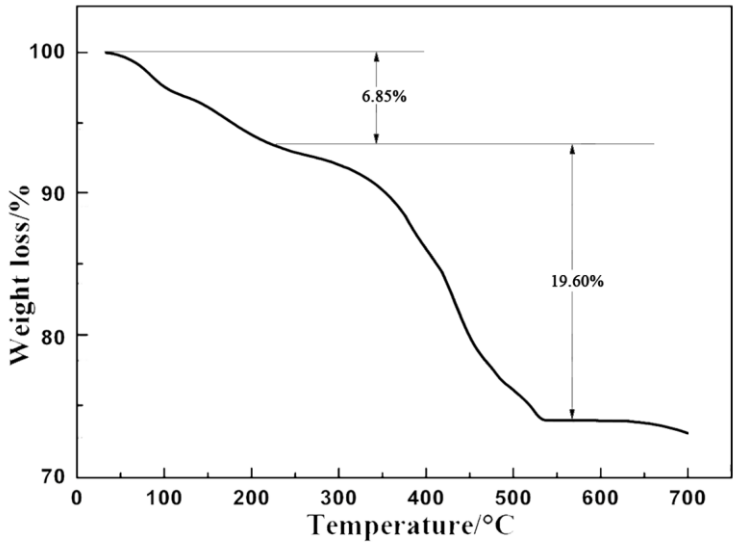

Fig. S12 TG curve of compound **2**

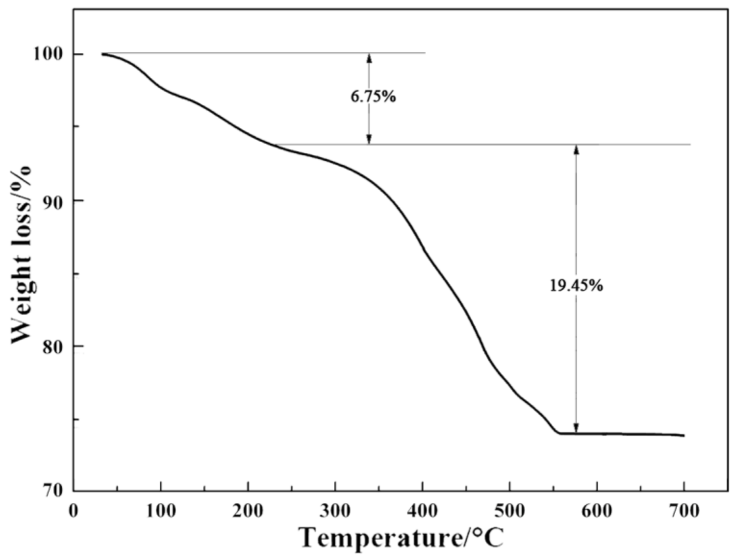

Fig. S13 TG curve of compound **3**